

High Frequency Parasitic Effects for On-Wafer Packaging of RF MEMS Switches

Alexandros Margomenos¹, and Linda P. B. Katehi²

¹Radiation Laboratory, Electrical Engineering and Computer Science Department, University of Michigan, 1301 Beal Avenue, Ann Arbor, MI 48109-2122, USA.

²School of Engineering, Purdue University, West Lafayette, IN 47907, USA.
amargome@engin.umich.edu, katehi@purdue.edu.

Abstract— A silicon micromachined on-wafer DC to 40 GHz packaging scheme for RF MEMS switches is presented. The designed on-wafer package has an insertion loss which is less than 0.3 dB up to 40 GHz (including a 2.7 mm long through line) and a return loss below -18 dB up to 40 GHz. The inclusion of the bonding ring and the dc bias lines creates parasitic resonances. This paper presents a detailed study of the package parasitics and provides solutions that can effectively eliminate them for frequencies up to 40 GHz

I. INTRODUCTION

IN the last decade the maturity of surface and bulk micromachining enabled the development of microelectromechanical systems (MEMS). In the RF area MEMS are mainly used as switches that utilize mechanical movement to achieve a short or an open circuit in a RF transmission line. While excellent performance has been reported for these devices, their operation is very sensitive to environmental factors, such as humidity and small particles. Therefore their integration to real-life systems can be problematic without a low-cost, low-loss hermetic package. Until recently the only concern when designing RF packages was the value of the return loss. However, as the operating frequencies became higher, design for packaging schemes became more demanding since the performance requirements for good RF response are very stringent. Poor design and fabrication can lead to increased cavity resonances and cross-talk between neighboring circuits while accessing the packaged device should be performed with low insertion and return loss. Additionally, on-wafer packaging architectures suffer from high frequency parasitic effects due to the coexistence of the encapsulating device, via-holes, bias lines and feeding interconnects on a single wafer. This paper presents an attempt to address these effects for the RF MEMS packaging architecture introduced in [1].

II. PACKAGED RF MEMS SWITCH

A low actuation voltage RF MEMS switch has been developed at the University of Michigan and tested to demonstrate actuation voltages as low as 6 Volts and an isolation of -26 dB at 40 GHz. The on-to-off capacitance ratio is 48, while power handling measurements show no "self-biasing" or failure for power levels up to 6.6 W at X-band. The operation of the switch requires DC as well as RF interconnects which carry the DC voltage and RF current from the probe pads to the device. In the on-wafer packaging archi-

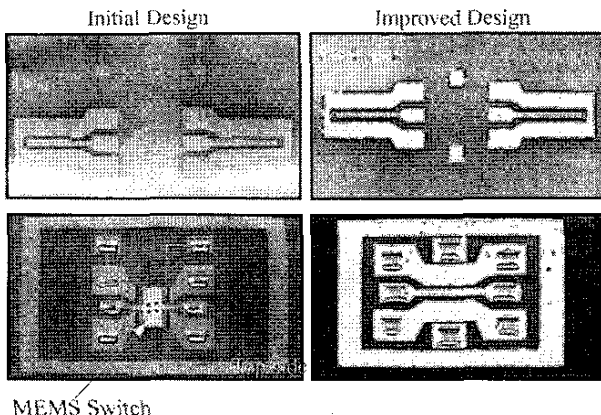


Fig. 1. Scanning electron image of packaged RF MEMS switch and improved RF transition.

ecture introduced in [1] the DC and RF pads are printed on the opposite side of the Si wafer that carries the switch and are then transitioned via appropriate through-wafer transitions designed to operate well both for DC and RF signals. A scanning electron image of the packaged MEMS device suspended over the RF transition is presented in Fig. 1. Its performance is illustrated in Fig. 2, where both the ON and OFF states of the switch are shown. The insertion loss of the transition (including a 2.7 mm though line) is 0.4 dB up to 40 GHz. The return loss at higher frequencies is increased due to the capacitance introduced by the switch but it is below -10 dB up to 40 GHz. When the switch is in the ON position its capacitance increases to 1.9 pF (as can be extracted from the S-parameters) and the measured isolation is approximately -23 dB at 40 GHz. These measured results illustrate that the broad bandwidth of this package renders it applicable for both low and high frequency MEMS devices.

As can be observed from Fig. 2 the measured response of the RF transition introduced four parasitic resonances at 8,14,22 and 28 GHz. These resonances are independent of the MEMS switch, since they occur even when a simple back-to-back transition is measured, and appear consistently in all the samples. Using a commercially available finite element solver [2] a theoretical analysis of the structure was performed which revealed the existence of two

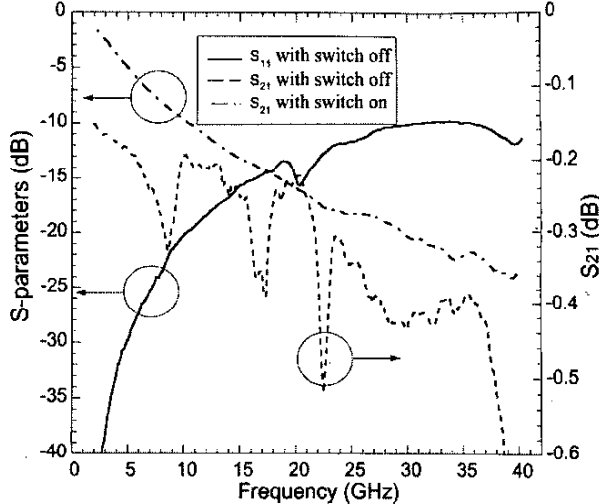


Fig. 2. Measured response of packaged RF transition and MEMS switch.

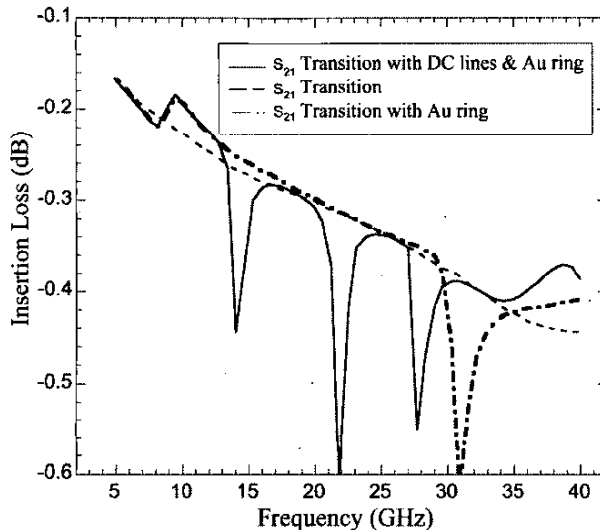


Fig. 3. Simulated results for RF transition.

mechanisms causing these parasitic effects: the gold bonding ring that surrounds the structure and the DC bias lines that are used for the activation of the switch.

The idea of an on-wafer packaging scheme implies that a sealing ring will be created on the same wafer with the structure that is encapsulated. Since hermeticity is a basic requirement for MEMS packaging Au eutectic bonding was the method selected for sealing the package. However, a metallic square ring resonates at the frequencies where its total length equals a wavelength and for the structure under consideration this occurs at 8 and 28 GHz. This result can be clearly observed in Fig. 3 where some of the simulated results acquired are presented. In this graph the response of the transition without the gold ring and the DC bias lines, along with the two cases where these elements are added, is shown. The initial case, where only

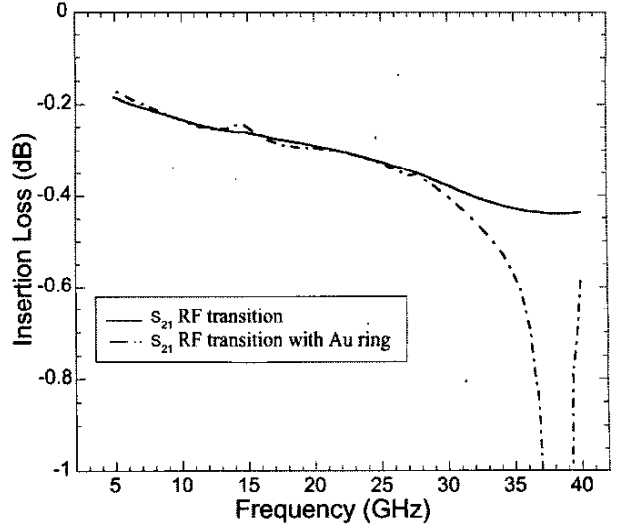


Fig. 4. Simulated results for improved RF transition.

the back-to-back transition is solved, illustrates no parasitic resonances and a total insertion loss that very closely approximates the measured result in Fig. 2. Subsequently, the Au ring was added and two resonances at 8 and 28 GHz appeared. One method for eliminating this effect is by reducing its total length and thus, pushing the resonances at higher frequencies. In the new transition, which will be presented below, this method was utilized. The ring was reduced at 1.7x1.8 mm and the parasitic effect of the ring was pushed to 38 GHz. This result is illustrated in Fig. 4 where the simulated response of the new transition is presented. The graph includes both a single RF transition (with the addition of the DC vias and bias lines) and the same transition with the Au bonding ring.

As was mentioned earlier DC lines are responsible for parasitic effects with resonances exhibited at 14 and 22 GHz. In particular the problems are caused by the line that connects one of the DC vias to the ground plane of the FGC line. This connection is required for the activation of the switch, since it creates the necessary voltage difference between the FGC line and the suspended air-bridge. As can be observed in Fig. 3 the addition of the bias lines creates the two resonances at 14 and 22 GHz. Varying the length of these lines (effectively changing the distance between the DC vias and the FGC ground plane) moves the resonances by as much as 4 GHz. By analyzing the structure with just the DC vias (no bias lines present) it was deduced that the vias themselves cause no parasitic effect. The addition of the bias line that connects one of the DC vias to the anchor point of the switch caused no resonance as well. When the bias line that connects to the FGC ground plane was added the two resonances at 14 and 22 GHz appeared. Therefore, it is presumed that this parasitic effect is caused by a resonance created by the bias line (on both the front and the back-side of the wafer) and the FGC ground plane. The two mechanisms that cause the parasitic effects are convoluted and therefore

a single solution that addresses both has to be found. The ring needs to surround both the top FGC line and the two DC vias and bias lines. Therefore the placement of the DC vias controls the length of the ring. The optimum results, presented in Fig. 4, were acquired when the two DC vias were placed in opposite sides and in close proximity to the RF transition. Thus, both the DC bias lines and the Au bonding ring have the minimum possible length. A scanning electron image of the new transition is shown in Fig. 1. In Fig. 5 the field distribution inside the dielectric is presented. As can be observed from the graph the field is stronger along the FGC line. However, a very strong field is launched by the edge of the dc bias line. The field concentrated at the Au bonding ring is -15 dB and the coupling seems to occur at the areas where the FGC line crosses below the ring. Moreover, due to the asymmetry of the structure the coupled field is more intense on the lower part of the ring compared to the top.

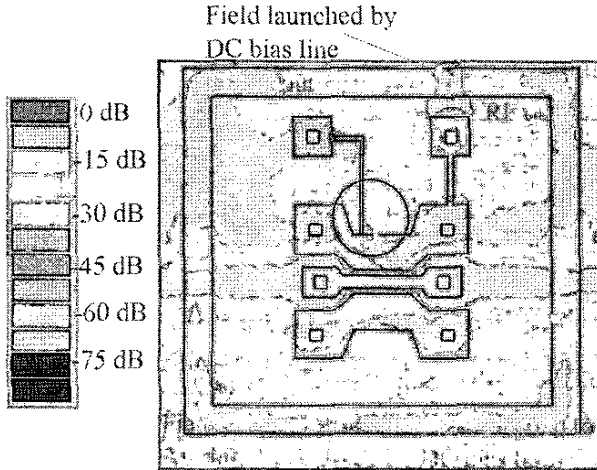


Fig. 5. Magnitude of the electric field underneath the Au bonding ring and the top FGC line.

III. FABRICATION PROCESS

Fabrication of the RF package is a multiphase process involving both surface and bulk micromachining. The samples used are 100 μm thick high-resistivity double-side polished silicon wafers, with 8700 \AA of SiO_2 thermally grown on both sides to allow for dual side processing. The main fabrication steps were described in detail in [1] where the initial packaging structure (Fig. 1) is introduced. The process analyzed in the referenced paper was optimized with respect to the final thickness of the deposited metal. The deposition technique used, which was introduced in [3], allows the simultaneous metallization of the side wall of the vias and the top FGC line via a "modified" lift-off. However, the final thickness of the metal can not exceed 1 μm due to the photoresist utilized. This thickness is adequate for W-band operation where the skin depth is approximately 0.25 μm , but insufficient for K band operation (skin depth of 0.5 μm at 20 GHz). Therefore the measured RF loss presented in [1] can be potentially reduced. Instead

of a lift-off the metallization is now achieved by sputtering a thin seed layer of Cr/Au immediately after the vias are anisotropically etched in potassium hydroxide (KOH), thus making sure that no native oxide is created on the lower walls of the via-holes. The use of a sputtering machine also ensures a more uniform coverage of the via sidewalls. Subsequently, 4 μm of Au are electroplated to form the FGC line. During the electroplating step the vias are also metallized along with the square ring of Cr/Au which is deposited around each circuit in order to be used for thermocompression bonding. The final metal thickness is larger than the skin depth even at the lower frequencies of operation and therefore the RF performance of the transition can be improved. In parallel with this the thicker metallization addresses a different weakness of the original design in which the hermeticity of the sealing was threatened by the thin metallization of the via walls. The lower walls of the via-hole transitions were approximately 2 μm thick (1 μm of Cr/Au from each side) and humidity could diffuse inside the packaging cavity. By increasing the metal thickness on the via walls the sealing quality can be significantly improved.

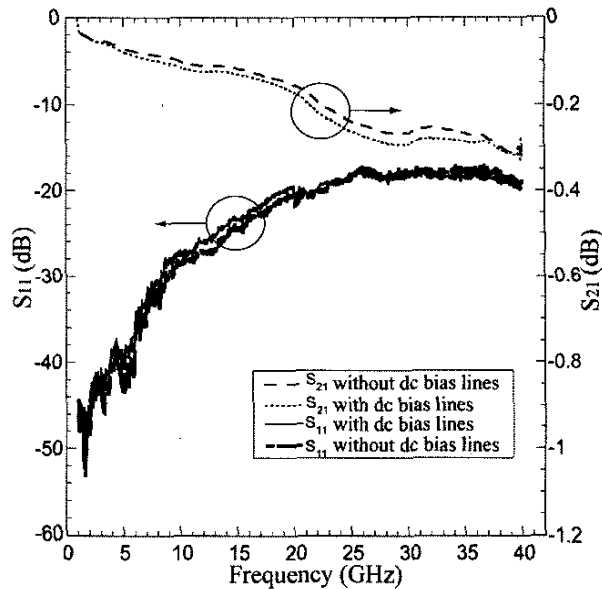


Fig. 6. Measured response of RF transition with and without DC bias lines and vias.

IV. MEASURED RESULTS

The measured response of the vertical back-to-back RF transition is displayed in Fig. 6. In order to demonstrate that the effects of the dc bias lines have been removed two cases are included in this figure. The transition is measured by itself and subsequently the dc vias and bias lines are added. By comparing the two results it is obvious that the addition of the bias lines has almost no effect on the RF response of the package. The measurements summarized in the figure include a 2.7 mm through line; therefore the total insertion loss is around 0.3 dB at 40 GHz. If the losses

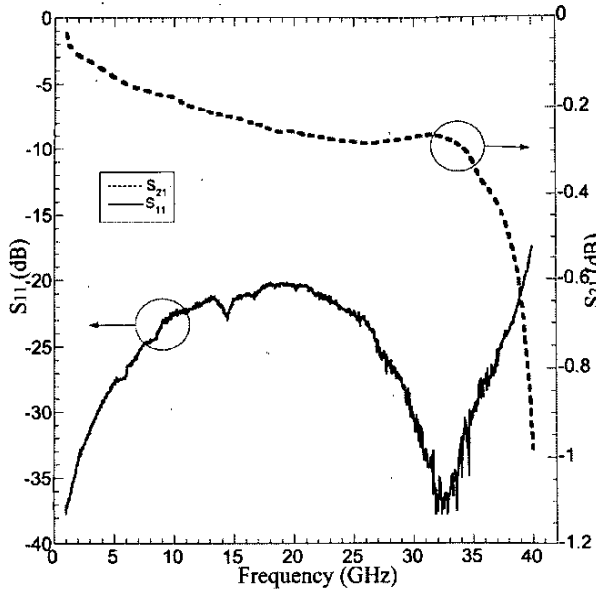


Fig. 7. Measured response of RF transition including the Au bonding ring.

from the FGC feeding lines are deembeded, the transition demonstrates a 0.06 dB loss up to 40 GHz and thus the loss due to each individual via transition is insignificant and approximately 0.03 dB. Taking into account the fact that no external wire bonding is needed in order to achieve signal propagation, this is the only loss introduced by the package. Additionally, the return loss is below -18 dB up to 40 GHz and therefore the transition is applicable for operation even higher than 40 GHz.

In the subsequent figure (Fig. 7) the measured results of the transition including the bonding ring are presented. As was previously mentioned the reduction of its length moved the resonant frequency at 38 GHz. As can be observed from the graph the measurement very closely approximates the theoretical expectation. The inclusion of the bonding ring reduces the operational bandwidth of the package below 40 GHz. However, if a non-hermetic or polyimide sealing is utilized (for non-MEMS applications) the package can be operated at higher frequencies.

V. HERMETICITY TESTING

A suitable package for encapsulation of RF MEMS needs to offer both exceptional RF performance and hermetic sealing. In order to test for hermeticity, the environment inside the package must be monitored for moisture penetration. This can be done by incorporating a dew point sensor inside the package and performing accelerated testing in an autoclave chamber. The dew point sensor is based on an interdigitated structure and has been previously used for lifetime testing of hermetic packages ([4], [5]). The operating principle is based on a large impedance change between the closely spaced electrodes of the sensor, which can be detected outside of the package through the via-holes. Once moisture condenses on the whole surface of the electrodes,

the total impedance of the dew point sensor will decrease. The structure is simple, compatible with the fabrication technology used and has good sensitivity. A scanning electron image of the fabricated sensor is presented in Fig. 8. The results of the accelerated testing, which will be included in the final paper, will allow the prediction of the lifetime of the package by evaluating its mean time to failure (MTTF) and activation energy.

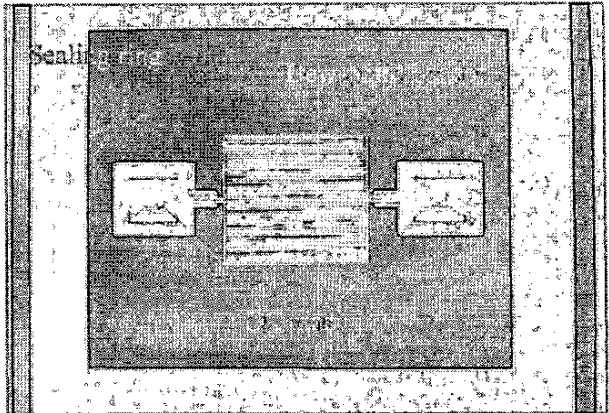


Fig. 8. Scanning electron image of dew-point sensor.

VI. CONCLUSIONS

We have demonstrated an on-wafer packaging scheme for RF MEMS switches. In order to address some high frequency parasitic effects a theoretical study has been performed and a new design was created following an improved fabrication process. The measured results showed excellent performance (insertion loss of 0.3 dB and return loss of -18 dB at 40 GHz) and no resonances up to 38 GHz. Accelerated testing of the package in an autoclave chamber is underway.

VII. ACKNOWLEDGEMENTS

The authors will like to thank D. Peroulis for the fabrication of the RF MEMS switch. This work was supported by the U.S. Army Research Laboratory under contract number DAAD-19-01-2-0008.

REFERENCES

- [1] A. Margomenos and L.P.B. Katehi, "DC to 40 GHz On-Wafer Package for RF MEMS Switches," *IEEE Topical Meeting on Electronic Performance of Electronic Packaging, Digest of Papers*, pp. 91–94, October 2002.
- [2] Ansoft Version 8.0, *High-Frequency Structure Simulator*, 2001.
- [3] K.H. Herrick, J.-G. Yook, S.V. Robertson, G.M. Rebeiz, and L.P.B. Katehi, "W-band Micromachined Vertical Interconnection for Three-Dimensional Microwave ICs," in *29th European Microwave Conference Proceedings*, Munich, Germany, October 1999, pp. 402–405.
- [4] B Ziaie, J.A. Von Arx, M. Dokmei, and K. Najafi, "A Hermetic Glass-Silicon Micropackage with High-Density On-Chip Feedthroughs for Sensors and Actuators," *Journal of Microelectromechanical Systems*, vol. 5, pp. 166–179, 1996.
- [5] M.G. Kovac, D. Chleck, and P. Goodman, "A New Moisture Sensor for In-Situ Monitoring of Sealed Package," *Proc. Int. Reliability Physics Symposium*, pp. 85–91, 1977.